



SUB-SYNCHRONOUS RESONANCE FREQUENCY EFFECT On STATCOM SMALL-SIGNAL MODEL And STABILITY ASSESSMENT MEASURES

Khaled Abojlala

Electrical and Electronic department, Faculty
of Engineering, Misurata University

Abstract— Sub-synchronous resonance (SSR) is a well-known phenomenon caused by power exchange between the network and the mechanical part of the generators. The STATCOM controller is a type of shunt FACTS devices employed to compensate the SSR and provide the necessary dynamics to the system. Investigating their contribution to the network requires a good representation of the STATCOM at different operating conditions. This paper presents two modelling techniques found in the literature, synchronous dq and dq-dynamic phasor modelling. The SSR frequency is included in the STATCOM model using a dq-dynamic phasor and compared with conventional dq modelling. The modelling is carried out for the small signal stability assessment techniques, while the validation is done using the time domain model under MATLAB/Simulink environment. In addition, the paper discusses the suitability of different stability measures to identify the stable operation of the STATCOM using the two derived models. The paper presented the suitability of criteria-based transfer functions to assess the SSR effect with the ability to track small signal changes.

Index Terms— Sub-synchronous resonance -STATCOM-dq model- dq dynamic phasor model – Impedance -Eigenvalue.

I. INTRODUCTION

Improving the power transfer capability of long transmission lines is subjected to reduce the effective line reactance by series or shunt compensators for example [1][2]. The series compensators of long transmission lines provide the most economical way and an effective means of reducing the line reactance, however, the connection of these compensators with the network might cause an exchange of power between the network and the generator. This power exchange is called sub-synchronous resonance (SSR). It is defined as a condition of the power system where the network exchanges energy at one or more frequencies with the turbine generator of the combined system under synchronous system frequency[3][4]. Although the dynamic interaction has

effect of the SSR[5]. In a traditional power system, the

steady-state SSR is based on two physical effects: the induction generator effect and torsional interaction. The former effect reduces the total stator resistance and consequently increases the time constant to decay the exciting torque, while the latter causes a negative time constant which amplifies the electrical torque during the oscillations[7]. In the meantime, the transient SSR is based on torque amplification or called shaft torque amplification that follows significant disturbances[8].

Choosing modelling technique of the systems has a important influence on presenting the generated oscillatory, and consequently the evaluation of the compensation technique. In the literature, some analytical programs such as EMTP implements time domain models that are utilised to study and analyse the SSR effect. However, such programs introduce little insight into the system[9]. Meanwhile, dq-based models are the commonly used coordinate to analyse the SSR and oscillations on the power system in other programs. However, it cannot represent all the harmonic frequencies that appeared on the system which might affect the design of different power components.

Fourier coefficient used by dynamic phasor provides the possibility to include the frequencies of interest in the studies. It was proposed first in 1991 for modelling power conversion circuits[10]. Slowing down the system states is a very useful feature introduced by dynamic phasor modelling. It improves the accuracy of the system linearisation during the high non-linearity of the SSR phenomenon[11]. The inclusion of harmonics increases the complexity of the model equations, however, it might be reduced by selecting appropriate frequencies associated with the study and deducting the less affected ones.

The SSR effect on stability assessment is commonly studied in the literature using different techniques that vary in accuracy and complexity, for instance, eigenvalue analysis [8][12], frequency scanning, small signal impedance [13]or fast Fourier transform (FFT) analysis[13].

Received 5 Oct, 2023; revised 25 Dec, 2023; accepted 30 Dec 2023.

Available online 31 Dec, 2023.

The eigenvalue analysis is a common and fast technique implemented to assess the system's performance. The benefits of using eigenvalue analysis are the analysis can present system instability and the existing oscillations for the studied network. In [14], the eigenvalue technique was applied to understand the sub-synchronous (SSR) effect of a system containing a synchronous machine connected to an infinite bus via a series compensated line. The authors applied the eigenvalue-based dynamic phasor to analyse the compensation using passive phase balance, by analysing their effect on the torsional modes of a turbine-generator system. Even though the system was analysed using the dynamic phasor, the inclusion of the fundamental frequency only reduces the advantage of the dynamic phasor model.

Alternatively, the small signal impedance assesses the stability at the point of connection, it uses the phase margin and Nyquist plots to predict system oscillations. The advantage of the small signal impedance method over the eigenvalue analysis is that the impedance analysis is both powerful and practical, especially in real-world applications when creating a fully detailed model of the power network becomes a challenging task [15][16]. The impedance analysis was carried out in [17], the paper implemented the ABC analysis of the dynamic phasor model at the fundamental frequency of a line connected to a double-fed induction machine (DFIG). The effective reactance was reduced by a thyristor-controlled series capacitor(TCSC). The paper compared the identified resonance frequency using ABC coordinates with an ABC-dynamic phasor. It indicated that the sets of frequencies for the dynamic phasor model are complemented by the time domain frequency due to the frequency shift caused by the dynamic phasor. The drawback of such analysis is not adequate to be compared with the dq impedances and stability criteria. In addition, the formulation of the diagonal impedances as pure real impedance quantities and pure imaginary impedances is completely ambiguous. In reality, all the impedances are in a complex form which deteriorates the use of such analysis using ABC dynamic phasor.

The stability measures based on impedance are classified into two categories; the first is magnitude-based models such as impedance norms and electrical damping, while the second category is based on transfer functions such as right-hand poles and Nyquist criteria. The former type is less sensitive to small system changes while the latter can identify the stability under different conditions.

The stability criteria-based impedance norms is a well-known technique in the literature. It examines whether or not the product of generator impedance and system admittance encircles the point (-1, 0) in the complex plane. It was first introduced in [18] and [19] to assess the AC system stability. The stability norms of the two sides of the system are utilised to assess the stability of the studied system.

The use of impedance matrix poles (or minor-loop gain) as a comparison with eigenvalue analysis was presented in [20] and[21]. The first paper presented the ability of impedance matrix poles to assess the local stability of HVDC system. In the meantime, the second paper presented a limitation of the impedance matrix poles which is the observability of the system is less than

the eigenvalue analysis. Such a one limited the impedance to identify the stability of the HVDC system in some cases. Alternatively, the eigenvalue analysis was not able to identify the system sustained harmonic oscillations caused by the voltage source converter (VSC) of the HVDC system.

Different methods have been proposed in the literature to reduce this interaction and eliminate SSR effect on the network. Flexible alternating current transmission system (FACTS) devices are the most common solution for the SSR behaviour such as static series compensators and static shunt compensators. In this paper, the static synchronous compensator (STATCOM) connected to a voltage source is modelled here as an example to model and analyse the SSR phenomenon, and assess the suitability to use different stability measures to study the SSR effect. The main sections of this paper are listed as follows:

- The derivation of the state space equations and derive the impedance matrix of STATCOM in synchronous dq coordinates.
- The validation of the dq model using MATLAB/Simulink time domain model.
- The derivation of the state space and impedance dq-dynamic phasor model of STATCOM in the presence of SSR frequency.
- The assessment of different stability measures and their suitability to identify the stability boundaries of the system, and present a comparison between the two models of the STATCOM.

II. DYNAMIC PHASOR CONCEPT

Dynamic phasor modelling (DP) was developed based on generalised average modelling using the time-varying Fourier coefficient in complex form. The complex periodic waveform $x(\tau)$ defined during the interval $\tau \in (t - T, t)$ using Fourier series as[10] [22]:

$$x(\tau) = \sum_{k=-\infty}^{\infty} X_k(t) e^{jk\omega_s\tau} \quad (1)$$

The ω_s represents the angular frequency of the system, k is the harmonic order of the signal and $X_k(t)$ represents the complex Fourier coefficient ‘‘dynamic phasor parameter’’ of the periodic signal which can be determined from(2).

$$X_k(t) = \frac{1}{T} \int_{t-T}^t X(\tau) e^{-jk\omega_s\tau} d\tau = x_k \quad (2)$$

The transformation requires the help of two other properties to solve a system using a dynamic phasor model which are:

- The dynamic phasor of a derivative of the time variable is:

$$\left\langle \frac{dx}{dt} \right\rangle_k = \frac{d(x)}{dt} + jk\omega_s \langle x \rangle_k \quad (3)$$

- The product of two-time domain variables is

$$\langle xy \rangle_k = \sum_{i=-\infty}^{\infty} \langle x \rangle_{k-i} \langle y \rangle_i \quad (4)$$

Analysing systems using the dynamic phasor concept is done by applying equations (1) to (4) to transform system time domain quantities to the dynamic phasor form and truncate less affected frequencies to represent dominant ones. The studied systems can be wholly or

partially transformed into dynamic phasor. The partial implementation is based on transforming the quantities of inductance and capacitor instead of the full transformation of system quantities [23].

III. DQ MODELLING OF STATCOM

The basic structure of STATCOM connected to a power network is demonstrated by a schematic diagram shown in Fig1.a. The STATCOM is modelled as resistance-inductance (RL) behind the voltage source. The MIMO control of STATCOM contains four proportional-integral (PI) controllers, feedforward bus voltage and decoupling control as shown in Fig1.b. The function of decoupling control is to cancel the cross-coupling between d and q coordinates, compensate the decoupling from the grid and the converter operation, and, improve the disturbance elimination capability of the STATCOM [24][25][26]. The input of the voltage control loop in the STATCOM controller is the DC voltage and the AC voltage. It provides direct control of the active and reactive power supplied or consumed by the STATCOM. In this paper, the system voltage and STATCOM voltage are assumed to be aligned. Therefore, the phase-locked loop (PLL) effect is ignored.

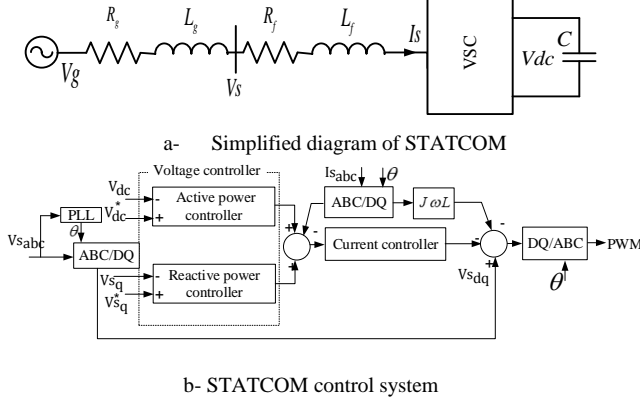


Figure 1. STATCOM construction and control

Based on the current directions assumed in Fig.1.a, the current equation of the STATCOM power circuit can be written as follows:

$$\frac{d}{dt} \mathbf{i}_{sdq} = \frac{1}{L_f} \mathbf{V}_{sdq} - \frac{R_f}{L_f} \mathbf{i}_{sdq} - \frac{V_{dc}}{L_f} \mathbf{m}_{sdq} + \beta \omega \mathbf{i}_{sdq} \quad (5)$$

Where (R_f, L_f) represent the STATCOM resistance and inductance. (v_s, i_s) represents the terminal voltage and the current as shown in Fig.1.a.

Using Fig.1.b the modulation index is equal to:

$$\mathbf{m}_{sdq} = \mathbf{V}_{sdq} - K p_{idq} (\mathbf{i}_{sdq}^* - \mathbf{i}_{sdq}) - \mathbf{x}_{1,2} + \omega L_f \mathbf{i}_{sdq} \quad (6)$$

$$\mathbf{x}_{1,2} = K i_{idq} \int (\mathbf{i}_{sdq}^* - \mathbf{i}_{sdq}) dt \quad (7)$$

The suitability of the external controller's inputs depends on the grid stiffness and its topology, as well as the purpose of the analysed converter. For weak grids, the suitable inputs are the DC link voltage and the magnitude of the terminal voltage of the controlled bus bar for the voltage control loops of STATCOM [27].

$$\mathbf{i}_{sdq}^* = K p_{vdq} (\mathbf{v}^* - \mathbf{v}) + \mathbf{x}_{3,4} \quad (8)$$

$$\mathbf{x}_{3,4} = K i_{vd} \int (\mathbf{v}^* - \mathbf{v}) dt \quad (9)$$

Similar relations can be derived from the outer control loop in case of active and reactive power is used instead of DC and AC voltages for other applications.

The DC side of STATCOM is controlled by the power balance equation which equals to:

$$P_s - P_{sdc} - P_{Loss} = 0 \quad (10)$$

By replacing the active power (P_s), the DC power (P_{sdc}) and losses (P_{Loss}) by their quantities to have the following differential equation:

$$\frac{3}{2} \mathbf{V}_{sdq}^T \cdot \mathbf{i}_{dq} - C \cdot V_{dc} \cdot \frac{d}{dt} V_{dc} - i_s^2 \cdot R_f = 0 \quad (11)$$

The (V_{dc}) and (C) represent the DC voltage and capacitor of the STATCOM.

By applying a small perturbation on the equations from (5) to (11) for linearisation, the state space equation of the STATCOM in the dq frame is:

$$\frac{d}{dt} \Delta \mathbf{X} = \mathbf{A}_{dq} \Delta \mathbf{X} + \mathbf{B}_{1dq} \Delta \mathbf{V}_{dq} + \mathbf{B}_{2dq} \mathbf{v} \quad (12)$$

$$\Delta \mathbf{i}_{dq} = \mathbf{C}_{dq} \mathbf{X} \quad (13)$$

$$\mathbf{X} = \begin{bmatrix} \Delta \mathbf{x}_{1,2} \\ \Delta \mathbf{x}_{3,4} \\ \Delta \mathbf{i}_{sdq} \\ \Delta V_{dc} \end{bmatrix}, \mathbf{v} = \begin{bmatrix} V_{dc}^* \\ V_{s_q}^* \end{bmatrix}, \mathbf{x}_{1,2} = \begin{bmatrix} x_1 \\ x_2 \end{bmatrix}, \mathbf{x}_{3,4} = \begin{bmatrix} x_3 \\ x_4 \end{bmatrix}$$

$$\mathbf{i}_{dq} = [i_d \quad i_q], \mathbf{V}_{dq} = \begin{bmatrix} V_d \\ V_q \end{bmatrix}, \beta = \begin{bmatrix} 0 & 1 \\ -1 & 0 \end{bmatrix}$$

The eigenvalue analysis guarantees the small signal stability of the systems in case of all system eigenvalues are allocated on the left-hand side of the complex plane.

The small signal impedance of the STATCOM can be simply derived from linearising the equations (5) to (11) with a proper arrangement to have:

$$\Delta \mathbf{V}_{dq} = \mathbf{Z}_{dq} \Delta \mathbf{i}_{dq} - \mathbf{A} \mathbf{A}_{dq} \mathbf{v}^* \quad (14)$$

$$\mathbf{Z}_{dq} = \{\mathbf{d} - \mathbf{b}(\mathbf{d} + \mathbf{fgh}) - \mathbf{ch}\}^{-1} \{\mathbf{a} + \mathbf{ck} + \mathbf{b}(\mathbf{e} + \mathbf{fgk})\} \quad (15)$$

$$\mathbf{A} \mathbf{A}_{dq} = \{\mathbf{d} - \mathbf{b}(\mathbf{d} + \mathbf{fgh}) - \mathbf{ch}\}^{-1} \mathbf{bfg} \quad (16)$$

The impedance (\mathbf{Z}_{dq}) has the form as:

$$\mathbf{Z}_{dq} = \begin{bmatrix} Z_{dd} & Z_{dq} \\ Z_{qd} & Z_{qq} \end{bmatrix} \quad (17)$$

Different stability criteria found in the literature were developed based on impedance. The criteria were developed to assess the small-signal stability of the power network based on generator and load admittance in dq coordinates [28]. They are introduced to ensure the stability of the interface between the two systems as the infinite one norm which is derived based on the Nyquist criterion and has the form[16]:

$$\mathbf{Z} \mathbf{Y}_{\infty 1} = \|\mathbf{Z}_{g}^{dq}\|_{\infty} \|\mathbf{Y}_{NT}^{dq}\|_1 < 0.5 \quad (18)$$

IV. MOCEL VALIDATION

The derived model of the dq model is validated in time domain operation in comparison with MATLAB/Simulink detailed model. The transformation of ABC quantities to dq of the detailed model are aligned at $\omega t = 0$ degree behind the phase A which yields that all

same block diagram used for dynamic phasor impedance can be employed for the dq impedance (or fundamental dynamic phasor impedance) with the assumption that the SSR components are equal to zero. Eliminating the harmonics effect from the equations (19) to (23) will result a dq model of the STATCOM.

Comparing the equation (16) and (23) shows an increase in the number of the state space equations by six equations, and the size of impedance matrix will be (4×4). Moreover, adding another frequency to the study will increase the number of state space equations to become nineteen equations and to impedance matrix size to be (7×7).

VI. SIMULATION AND ANALYSIS OF THE DQ MODEL AND DQ-DYNAMIC PHASOR MODEL

A- Eigenvalue and Impedance anlaysis:

The test system including filter components and STATCOM are presented in Fig.1a. The parameters of the STATCOM and the system are listed in Table I. The two derived models are compared here using two methods: small signal impedance and eigenvalue analysis of state space equations.

TABLE I. TEST SYSTEM PARAMETERS

Parameter	Value	Parameter	Value
R_g	30 Ω	Ms_q	400
L_g	0.001mH	Kp_{id}	800
V_d	410	Ki_{id}	8000
V_q	0	Kp_{vd}	10
f_s	60 Hz	Ki_{vd}	0.001
R_f	0.5 Ω	Kp_{iq}	800
L_f	5e-3 H	Ki_{iq}	8000
C_{dc}	400e-6 F	Kp_{vq}	0.01
V_{dc}	1000V	Ki_{vq}	2
Ms_d	-14.3		

The appropriate choice to represent the SSR frequency is to select Fourier quantities ($k = 0, 0.6$). The AC and DC components that control the active and reactive powers of STATCOM are represented by ($k = 0$), while ($k = 0.6$) represents the SSR components appeared on the test system. So, the input voltage of the STATCOM including the SSR frequency can be written as:

$$v(t) = V_0 \cos(\omega t + \phi + p) + V_{0.6} \cos(0.6\omega t + \phi + p) \quad (26)$$

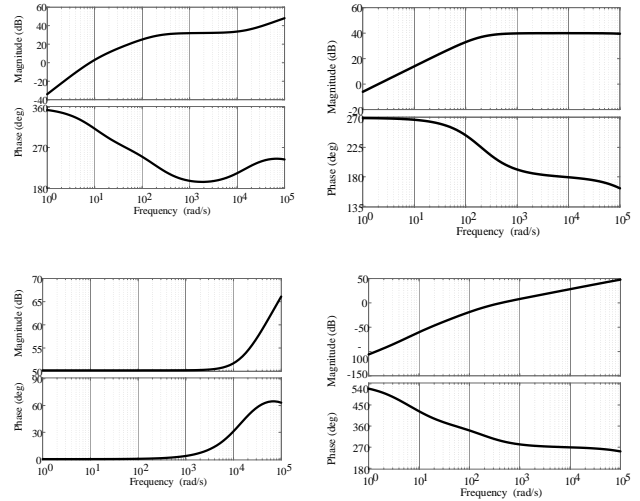
Hence: $p = (0, -\frac{2\pi}{3}, \frac{2\pi}{3})$ for phases (a, b, c) respectively.

The voltage equation presented in (26) has the following form in dynamic phasor:

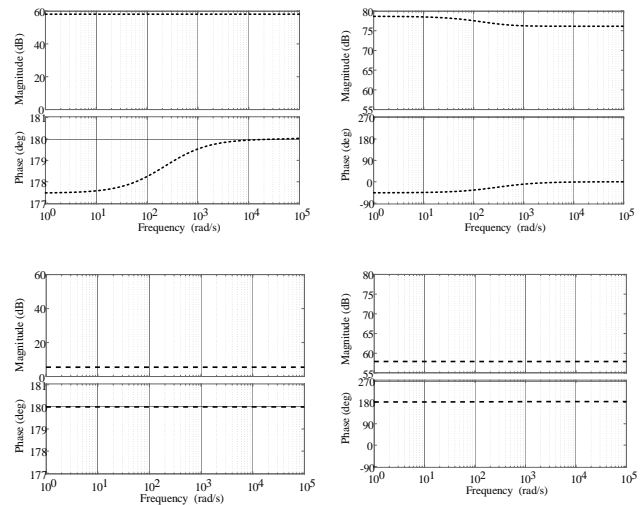
$$\langle V \rangle_0 = \frac{V_0}{2} e^{j(\phi+p)}, \langle V \rangle_{0.6} = \frac{V_{0.6}}{2} e^{j(\phi+p)} \quad (27)$$

Fig.4.a shows the small signal impedance of the STATCOM model at the subsynchronous frequency. The magnitude is almost constant for the four impedances except a slight change on for the (Zdq) impedance. Even though, the phase of the impedance is constant for the

(Zdq) impedance and (Zqq) impedance which are equal to 180°, the phase of (Zdd) and (Zqd) is changed from 177° and -45° at low frequency to become 180° and 0° at higher frequencies for the two impedances respectively.



a- Fundamental frequency impedance of STATCOM



b- The small signal impedance of STATCOM at SSR frequency

Figure 4. small signal impedance of STATCOM models

The small signal impedances at the fundamental frequency of the dq model presented the equation (16) and dq-dynamic phasor model including the SSR frequency presented in the equation (23) are plotted in Fig4.b.

Although the order of the dq impedances and the dq-dynamic phasor impedances at the fundamental frequency have different orders, both impedances have the same magnitude and phase over the range of plotted frequencies.

The diagonal impedances (Zdd) and (Zqq) have incremental increase over the frequency range. Alternatively, the off-diagonal impedances (Zdq) and (Zqd) have different behaviour. The (Zdq) increases gradually for frequencies lower than fundamental frequency and becomes constant for higher frequencies, while the (Zqd) is constant for the frequencies less than 3000 rad/sec and increases steadily for upper frequencies.

The second comparison in this section is made using the eigenvalues analysis by the STATCOM models in dq and dq-dynamic phasors coordinates of the state space equations (12) and (19). The aim of eigenvalue analysis of STATCOM dq and dq-dynamic phasor models is to identify the oscillatory modes of the models as well as identifying the participation factors of the model's modes which could contribute to the SSR frequency. As presented in the Table II,III, the dq model has (6) modes while the dq-dynamic phasor model has (12) modes.

The modes of the dq model of the test system have four frequencies (25.5MHZ, 2.45 kHz, 1.59×10^{-5} Hz and 1.59Hz). The associated damping ratio of all the STATCOM modes is about 100% which presents the ability of the STATCOM controller to damp these modes frequencies. The modes of dq model and participation factor are shown in Table II and III respectively. The dq model indicates that the modes frequencies have reasonable damping factors and doesn't indicate any instability or oscillatory modes.

TABLE II. EIGENVALUE DQ MODEL

λ	Eigenvalue-dq model	f_n (Hz)	Damping ratio (ζ)
λ_1	$-1.60 \times 10^8 + j3.77 \times 10^5$	2.55×10^7	100%
λ_2	$-1.60 \times 10^8 - j3.77 \times 10^5$	2.55×10^7	100%
λ_3	$-1.54 \times 10^4 + j0$	2.45×10^3	100%
λ_4	$-1.00 \times 10^4 + j0$	1.59×10^{-5}	100%
λ_5	$-10.00 + j0$	1.59	100%
λ_6	$-10.00 + j0$	1.59	100%

TABLE III. PARTICIPATION FACTOR OF DQ-MODEL

Mode	Δx_1	Δx_2	Δx_3	Δi_{sd}	Δi_{sq}	ΔV_{dc}
1	98.82%	98.82%	99.47%	0.00%	1.22%	1.22%
2	2.55%	2.55%	2.56%	0.12%	0.03%	0.03%
3	9.80%	9.80%	0.00%	0.00%	0.00%	0.00%
4	9.81%	9.81%	9.91%	99.50%	68.75%	72.36%
5	0.04%	0.02%	0.03%	0.23%	72.49%	68.89%
6	1.95%	1.95%	0.98%	9.95%	0.01%	0.01%

The eigenvalues of the STATCOM are calculated using the same parameters for the dq-dynamic phasor model including SSR frequencies. The modes of dq-dynamic phasor have seven frequencies (26.6MHz, 24.3MHz, 25.5MHZ, 2.45 kHz, 1.59×10^{-5} Hz, 1.59Hz and 36 Hz) as shown in Table IV and the participation factor in Appendix B. It is evident that the similarity between the frequencies found by the dq model with other interesting frequencies appeared using dq-dynamic phasor modes. The damping ratios of those similar frequencies have the same damping at about 100%.

Three new frequencies are appeared by the dq-dynamic phasor model which illustrates the behaviour of the STATCOM under the presence of the SSR frequency in dynamic phasor coordinates.

The first new frequency appeared by the dq-dynamic phasor mode (1) is 26.6MHz with damping frequency equal to 100%. These complex pairs are associated with DC voltage and the STATCOM dq-currents states. The main contribution of this mode is the DC voltage (ΔV_{dc})₀.

The second frequency mode appeared by the dq-dynamic phasor model (2) is 24.3MHz which is related to the current controller. The main contribution of this mode is an integral part of the PI controller of the current control loop at fundamental frequency state (Δx_1)₀. Moreover, the integral part of quadrature current state at SSR frequency (Δx_4)_{0.6} where the contribution factor is equal to 79.6% and 79.5% respectively and damping ratio equal to 100%.

The last frequency appeared by the dq-dynamic phasor model is 36Hz for modes (9, 10, 11 and 12) which show the inclusion of the SSR frequency will cause damped and non-damped oscillations by the same frequency at the output of the STATCOM as presented in Table.IV. The participation factor shows that the main contribution of this frequency is the integral part of the direct voltage loop at SSR frequency (Δx_3)_{0.6}. The real cause of this frequency is the frequency shift caused by the dynamic phasor transformation.

TABLE IV. EIGENVALUE DQ-DYNAMIC PHASOR MODEL

λ	Eigenvalue- dq dynamic phasor	f_n (Hz)	Damping ratio (ζ)
λ_1	$-1.67 \times 10^8 + j1.49 \times 10^8$	2.66×10^7	100%
λ_2	$-1.53 \times 10^8 + j1.13 \times 10^8$	2.43×10^7	100%
λ_3	$-1.54 \times 10^4 - j4.26 \times 10^{-14}$	2.45×10^3	100%
λ_4	$-1.60 \times 10^8 - j3.77 \times 10^5$	2.55×10^7	100%
λ_5	$-1.00 \times 10^4 - j8.77 \times 10^{-13}$	1.59×10^{-5}	100%
λ_6	$-10.00 + j1.17 \times 10^{-2}$	1.59	100%
λ_7	$-10.00 - j1.17 \times 10^{-2}$	1.59	100%
λ_8	$-1.60 \times 10^8 + j3.76 \times 10^5$	2.55×10^7	100%
λ_9	$-10.00 - j226.171$	36.03	4%
λ_{10}	$-10.00 - j226.218$	36.04	4%
λ_{11}	$0.00 - j226.195$	36.00	0%
λ_{12}	$0.00 - j226.195$	36.00	0%

B- System behaviour under change of parameters:

The move of the STATCOM eigenvalues over the change of control parameters is tested for the two models.

It is done by changing the same control parameters (k_{iid}, k_{ivd}). The two complex conjugate eigenvalues found on the system tend to become real values as the k_{ivd} increases. In the meantime, it is evident from Fig5.b that the two complex conjugate eigenvalues of the dq-dynamic phasor model tend to stay complex pairs over the same change. In the meantime, the change of the (k_{iid}) has the same effect on both models and drag the system to an unstable region as shown in Fig5.b and Fig5. c. Also, this change cause shifting the eigenvalue (36Hz) appeared on dq-dynamic phasor to become unstable by moving to the right-hand side. The powerful of the eigenvalue analysis is that the eigenvalues of both STATCOM models are presenting the same stability and the instability modes of the STATCOM models without considering the behaviour of these modes over the changes of the parameters.

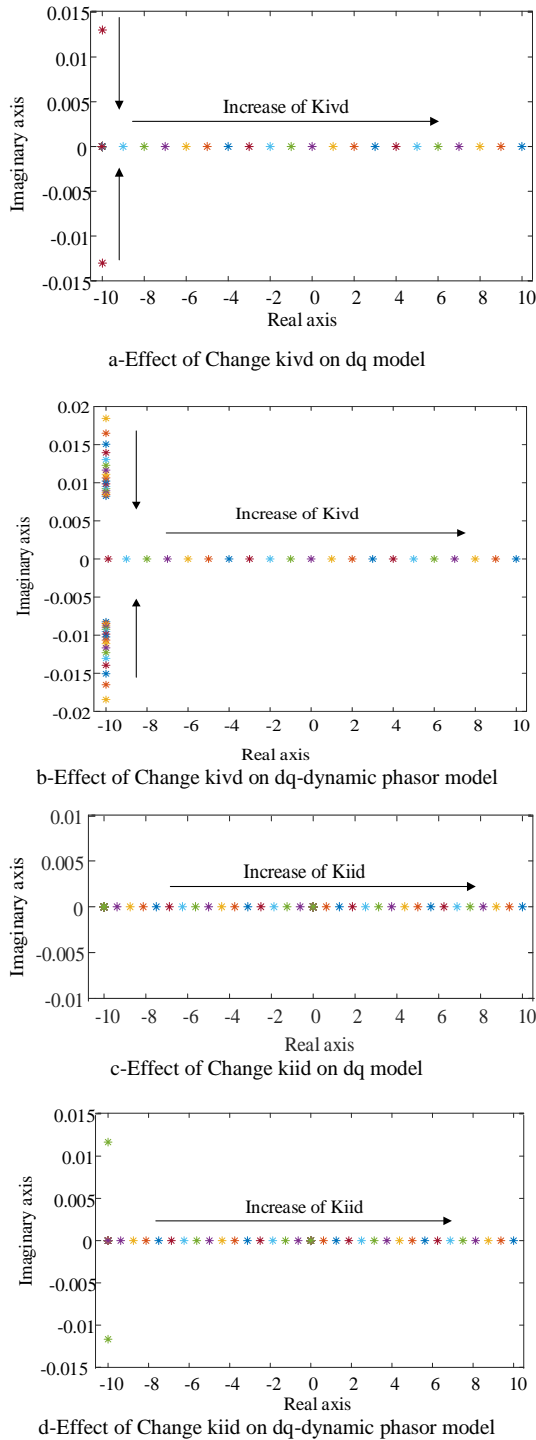


Figure 5. Effect of changing control parameters on dq-model and dq-dynamic phasor model

C- Stability norms of STATCOM models

The one-infinite norm stability criterion presented in the equation (18) is compared to both models as shown in Fig.6. The criterion ensures the stability of the system if the product of the two norms is less than the stability threshold 0.5 (-6.02dB).

The dq model and dq-dynamic phasor model at the fundamental frequency of the STATCOM has the same impedance norms as shown in Fig.6.a and Fig.6.b. In the meantime, the impedance norms at SSR frequency is presented in Fig.6.c and Fig.6.d.

Generalising the existence stability criteria-based norms are required to ensure the stability of the system in at fundamental as well as at the harmonic frequencies. The current stability criteria found in the literature are based impedance magnitude is the low sensitivity to the small changes of the devices/systems parameters. Another drawback of the stability criteria based norms that the criteria are sufficient for the stability but not necessary to ensure the system’s stability. Therefore, ensuring system stability can be guaranteed by other stability assessment tools such as right-hand poles (RHP) or Nyquist stability criterion where the device/system transfer function is considered. Further research will be carried out on this point in future publications.

D-Right-hand poles of STATCOM impedance matrix

A good view of the stability can be assessed using the poles of impedance matrix of dq-model and dq-dynamic phasor model. As presented in [27], the impedance matrix can be extracted from the state-space equations. Those equations should contain all the states of the system including the zero states. The impedance can be extracted using the following form:

$$YZ = C[sI - A]^{-1} B + D \tag{28}$$

The output of equation (28) can be impedance or admittance based on the inputs and the outputs of the system.

In this section, two control parameters are chosen to be varied between stable and unstable conditions. Those parameters are an integral part of the direct controller (*kiid*) and the integral part of direct voltage controller (*kivd*).

To test the two models: (*kivd*) is changed for three values [-8000, 0, 8000] as well as the (*kiid*) is changed for three values [-0.001,0,001].The change of the control variable (*kiid* and *kivd*) for dq-model presented in the equation (254) can be used as a measure of the stability of the device which shows the same effect on the impedance matrix poles. The stable eigenvalue of the STATCOM eigenvalues calculated by the equation (19) is seen as poles of the impedance matrix allocated at the left-hand-side of the complex plane.

The impedance matrix poles are repeated eigenvalues for the dq model and shifted for the dq-dynamic phasor model due to the nature of dq impedance which referred to the origin of both state space matrix and the impedance matrix.

Alternatively, the change of the control variable for the dq-dynamic phasor model presents the expected stable and unstable operating conditions of the STATCOM while the poles of impedance matrix of dq-dynamic phasor model show some right-hand poles even for the stable conditions. The main reason for the appearance of the RHP appeared is the inclusion of SSR frequency on the STATCOM model which is not found in the fundamental impedance matrix.

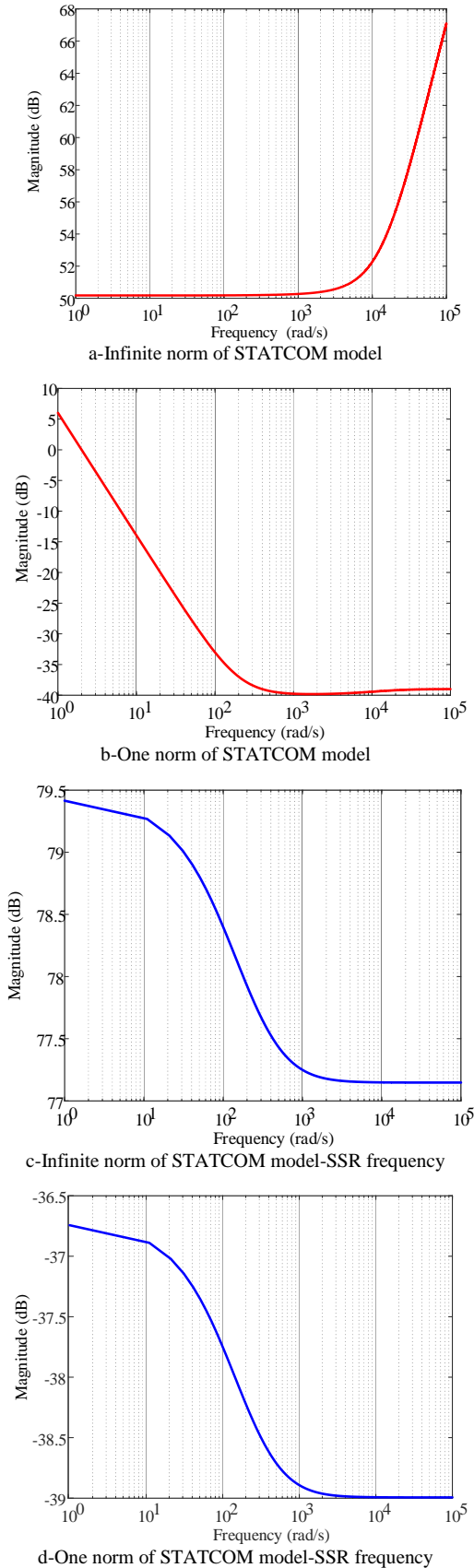


Figure 6. Comparison between the stability criteria of dq and dq-dynamic phasor models

VII. CONCLUSION

This paper discussed the presence of the SSR frequencies within the power networks modelling for

stability assessment. The paper investigated the STATCOM model in synchronous dq coordinates and dq-dynamic phasor including SSR frequency. The effect on both modelling techniques was examined in the small signal impedance and eigenvalue analysis. The fundamental impedance of dq-dynamic phasor model of the STATCOM has the same impedance magnitude as the dq model. Alternatively, the eigenvalue analysis of STATCOM model showed an increase in the number of modes by the STATCOM. Also, the dq-dynamic phasor modes presented the non-damped SSR frequency found on the modes caused by the frequency transformation of the dynamic phasor. The increase of the number of harmonics within the model tends to enhance the number of the equations and the states of the model. A further investigation about the adoption of the stability criteria including the harmonics and oscillations in dq-dynamic phasor, and the use of the dq-dynamic phasor model to design SSR dampers will be carried out in future research.

REFERENCES

- [1] M. R. R. Iravani, P. L. P. L. Dandeno, D. Maratukulam, K. H. H. Nguyen, D. Zhu, and D. Maratukulam, 'Applications of static phase shifters in power systems', *IEEE Transactions on Power Delivery*, vol. 9, no. 3, pp. 1600–1608, 1994, doi: 10.1109/61.311204.
- [2] X. Yuan et al., 'An effective control scheme for multimodal SSR suppression via VSC-based controller', *IEEE Access*, vol. 8, pp. 172581–172592, 2020, doi: 10.1109/ACCESS.2020.3025152.
- [3] N. Prabhu, M. Janaki, and R. Thirumalaivasan, 'Damping of subsynchronous resonance by subsynchronous current injector with STATCOM', *IEEE Region 10 Annual International Conference, Proceedings/TENCON*, pp. 1–6, 2009, doi: 10.1109/TENCON.2009.5395835.
- [4] Z. Zhu, J. Yan, C. Lu, Z. Chen, and J. Tian, 'Two-Stage Coordinated Control Strategy of AC/DC Hybrid Power System Based on Steady-State Security Region', *IEEE Access*, vol. 8, pp. 139221–139243, 2020, doi: 10.1109/ACCESS.2020.3012634.
- [5] A. Tabesh and R. Iravani, 'On the application of the complex torque coefficients method to the analysis of torsional dynamics', *IEEE Transactions on Energy Conversion*, vol. 20, no. 2, pp. 268–275, 2005, doi: 10.1109/TEC.2005.847970.
- [6] I. M. Canay, 'A novel approach to the torsional interaction and electrical damping of the synchronous machine: Part II: Application to an arbitrary network', *IEEE Transactions on Power Apparatus and Systems*, vol. PAS-101, no. 10, pp. 3639–3647, 1982, doi: 10.1109/TPAS.1982.317049.
- [7] A. E. Leon and J. A. Solsona, 'Sub-synchronous interaction damping control for DFIG wind turbines', *IEEE Transactions on Power Systems*, vol. 30, no. 1, pp. 419–428, 2015, doi: 10.1109/TPWRS.2014.2327197.
- [8] P. Mattavelli, 'Ssr analysis with dynamic phasor model of thyristor-controlled series capacitor', *IEEE Transactions on Power Systems*, vol. 14, no. 1, pp. 200–208, 1999, doi: 10.1109/59.744524.
- [9] S. R. Sanders, J. M. Noworolski, X. Z. Liu, and G. C. Verghese, 'Generalized Averaging Method for Power Conversion Circuits', *Power Electronics*,

- IEEE Transactions on, vol. 6, no. 2, pp. 251–259, 1991, doi: 10.1109/63.76811.
- [10] Y. Shujun, B. Mingran, H. Minxiao, H. Junxian, and W. Lei, ‘Modeling for VSC-HVDC Electromechanical Transient Based on Dynamic Phasor Method’, 2nd IET Renewable Power Generation Conference (RPG 2013), pp. 2.58-2.58, 2013, doi: 10.1049/cp.2013.1795.
- [11] A. Moharana and R. K. Varma, ‘Subsynchronous resonance in single-cage self-excited-induction-generator-based wind farm connected to series-compensated lines’, IET Gener. Transm. Distrib. (UK), vol. 5, no. 12, pp. 1221–1232, 2011, doi: 10.1049/iet-gtd.2010.0618.
- [12] Z. Miao, ‘Impedance-model-based SSR analysis for type 3 wind generator and series-compensated network’, IEEE Transactions on Energy Conversion, vol. 27, no. 4, pp. 984–991, 2012, doi: 10.1109/TEC.2012.2211019.
- [13] M. Bongiorno et al., ‘Single-phase VSC based SSSC for subsynchronous resonance damping’, IEEE Transactions on Power Delivery, vol. 23, no. 3, pp. 1544–1552, 2008, doi: 10.1109/TPWRD.2007.916231.
- [14] M. C. Chudasama and A. M. Kulkarni, ‘Dynamic phasor analysis of SSR mitigation schemes based on passive phase imbalance’, IEEE Transactions on Power Systems, vol. 26, no. 3, pp. 1668–1676, 2011, doi: 10.1109/TPWRS.2010.2072793.
- [15] C. Li, R. Burgos, Y. Tang, D. Boroyevich, and V. Tech, ‘Impedance-Based Stability Analysis of Multiple STATCOMs in Proximity’, in Compel2016, IEEE, Jun. 2016, pp. 1–6. doi: 10.1109/COMPEL.2016.7556744.
- [16] K. a. K. Corzine et al., ‘AC Impedance Measurement Techniques’, IEEE International Conference on Electric Machines and Drives, 2005., pp. 1850–1857, 2005, doi: 10.1109/IEMDC.2005.195972.
- [17] L. Piyasinghe et al., ‘Impedance model-based SSR analysis for TCSC compensated type-3 wind energy delivery systems’, IEEE Trans Sustain Energy, vol. 6, no. 1, pp. 179–187, Jul. 2015, doi: 10.1109/TSTE.2014.2362499.
- [18] M. Belkhat, ‘Stability Criteria for AC Power Systems with Regulated Loads’, 1997. doi: 10.1108/eb050773.
- [19] S. Chandrasekaran, D. Borojevic, and D. K. Lindner, ‘Input filter Interaction in Three Phase AC-DC Converters’, pp. 1–6, 1999.
- [20] ‘VSC-HVDC Systems’, Norwegian University of Science and Technology, Trondheim, Norway, 2008.
- [28] K. Corzine, M. Belkhat, Y. Familant, and J. Huang, ‘AC impedance measurement techniques’, 2005.

APPENDIX

Appendix A:

dq- model symbols and matrices

$$\mathbf{B}_{1dq} = \begin{bmatrix} 0 & 0 & 0 \\ -Ki_{iq}Kp_{vq} & 0 & 0 \\ 0 & 0 & 0 \\ \frac{1}{L_f} - \frac{V_{dc}}{L_f} & 0 & 0 \\ -\frac{V_{dc}}{L_f}Kp_{iq}Kp_{vq} & \frac{1}{L_f} - \frac{V_{dc}}{L_f} & \frac{V_{dc}}{L_f}Kp_{iq} \\ \frac{3}{2} \frac{is_d}{CV_{dc}} & \frac{3}{2} \frac{is_q}{CV_{dc}} & 0 \end{bmatrix} \quad \mathbf{B}_{2dq} = \begin{bmatrix} Ki_{id}Kp_{vd} & 0 \\ 0 & Ki_{iq}Kp_{vq} \\ Ki_{vd} & 0 \\ \frac{V_{dc}}{L_f}Kp_{vd}Kp_{id} & 0 \\ 0 & \frac{V_{dc}}{L_f}Kp_{iq}Kp_{vq} \\ 0 & 0 \end{bmatrix} \quad \mathbf{C}_{dq} = \begin{bmatrix} 0 & 0 & 0 & 1 & 0 & 0 \\ 0 & 0 & 0 & 0 & 1 & 0 \end{bmatrix}$$

$$b = \begin{bmatrix} V_{dc} & 0 \\ 0 & V_{dc} \end{bmatrix} \quad c = \begin{bmatrix} ms_d & 0 \\ ms_q & 0 \end{bmatrix} \quad e = \begin{bmatrix} Kp_{id} + \frac{Ki_{id}}{S} & \omega L_f \\ -\omega L_f & Kp_{iq} + \frac{Ki_{iq}}{S} \end{bmatrix} \quad h = \begin{bmatrix} \frac{3}{2} G_{dc} \frac{is_d}{CV_{dc}} & \frac{3}{2} G_{dc} \frac{is_q}{CV_{dc}} \\ \frac{CV_{dc}}{G_{dc}} & 0 \end{bmatrix} \quad f = \begin{bmatrix} Kp_{id} + \frac{Ki_{id}}{S} & 0 \\ 0 & Kp_{iq} + \frac{Ki_{iq}}{S} \end{bmatrix}$$

$$k = \begin{bmatrix} G_{dc} \frac{3}{2} \frac{Vs_d - 2is_d \cdot R_f}{CV_{dc}} & G_{dc} \frac{3}{2} \frac{Vs_q}{CV_{dc}} \\ 0 & 0 \\ 0 & 0 \\ \frac{V_{dc}}{L_f} & 0 \\ 0 & \frac{V_{dc}}{L_f} \\ 0 & 0 \end{bmatrix} \quad G_{dc} = \frac{CV_{dc}^2}{SCV_{dc}^2 - is_d^2 \cdot R_f + \frac{3}{2} Vs_d \cdot is_d + \frac{3}{2} Vs_q \cdot is_q} \quad d = \begin{bmatrix} 1 & 0 \\ 0 & 1 \end{bmatrix} \quad g = \begin{bmatrix} Kp_{vd} + \frac{Ki_{vd}}{S} & 0 \\ 0 & Kp_{vq} + \frac{Ki_{vq}}{S} \end{bmatrix}$$

$$\mathbf{A}_{dq} = \begin{bmatrix} 0 & 0 & Ki_{id} & -Ki_{id} & 0 & -Ki_{id}Kp_{vd} \\ 0 & 0 & 0 & 0 & -Ki_{iq} & 0 \\ 0 & 0 & 0 & 0 & 0 & -Ki_{vd} \\ \frac{V_{dc}}{L_f} & 0 & \frac{V_{dc}}{L_f}Kp_{id} & -\frac{R_f}{L_f} - \frac{V_{dc}}{L_f}Kp_{id} & \omega - V_{dc}\omega & -\frac{ms_d}{L_f} - \frac{V_{dc}}{L_f}Kp_{id}Kp_{vd} \\ 0 & \frac{V_{dc}}{L_f} & 0 & -\omega + V_{dc}\omega & -\frac{R_f}{L_f} - \frac{V_{dc}}{L_f}Kp_{iq} & -\frac{ms_q}{L_f} \\ 0 & 0 & 0 & \frac{3}{2} \frac{Vs_d - 2is_d \cdot R_f}{CV_{dc}} & \frac{3}{2} \frac{Vs_q}{CV_{dc}} & \frac{is_d^2 \cdot R_f - \frac{3}{2} Vs_d \cdot is_d - \frac{3}{2} Vs_q \cdot is_q}{CV_{dc}^2} \end{bmatrix} \quad a = \begin{bmatrix} SL_f + R_f & -\omega L_f \\ \omega L_f & SL_f + R_f \end{bmatrix}$$

- dq-dynamic phasor model parameters:

$$A_{DP} = [A1 \quad A2 \quad A3], \quad \alpha_{dc} = \langle \frac{1}{CV_{dc}^2} \rangle_0 \left\{ (is_d^2 \cdot R_f)_0 + \frac{3}{2} (-\langle Vs_d \rangle_{0.6} \langle is_d \rangle_{0.6}^* - \langle Vs_d \rangle_0 \langle is_d \rangle_0 - \langle Vs_d \rangle_{0.6} \langle is_d \rangle_{0.6} - \langle Vs_q \rangle_{0.6} \langle is_q \rangle_{0.6}^* - \langle Vs_q \rangle_0 \langle is_q \rangle_0 - \langle Vs_q \rangle_{0.6} \langle is_q \rangle_{0.6}) \right\}$$

$$E_2 = \omega L_f \cdot d G = \begin{bmatrix} Kp_{vd} + \frac{K_{i_{vd}}}{s} & 0 & 0 \\ 0 & 0 & 0 \\ 0 & Kp_{vq} + \frac{K_{i_{vq}}}{s} & 0 \\ 0 & 0 & Kp_{vq} + \frac{K_{i_{vq}}}{s+j0.6\omega} \end{bmatrix}$$

$$E = \begin{bmatrix} E_1 & E_2 \\ -E_2 & E_3 \end{bmatrix} F = \begin{bmatrix} E_1 & 0 \\ 0 & E_3 \end{bmatrix}$$

$$E_1 = \begin{bmatrix} Kp_{id} + \frac{K_{i_{id}}}{s} & 0 \\ 0 & Kp_{id} + \frac{K_{i_{id}}}{s+j0.6\omega} \end{bmatrix}$$

$$\beta = \langle V_{dc} \rangle_0 \cdot d C = \begin{bmatrix} \langle ms_d \rangle_0 \\ \langle ms_d \rangle_{0.6} \\ \langle ms_q \rangle_0 \\ \langle ms_q \rangle_{0.6} \end{bmatrix} (0)_{3 \times 4}$$

$$A2 = \begin{bmatrix} K_{i_{id}} & 0 & 0 \\ 0 & K_{i_{id}} & 0 \\ 0 & 0 & 0 \\ 0 & 0 & K_{i_{iq}} \\ 0 & 0 & 0 \\ 0 & -j0.6\omega & 0 \\ 0 & 0 & -j0.6\omega \\ \langle \frac{V_{dc}}{L_f} \rangle_0 Kp_{id} & 0 & 0 \\ 0 & \langle \frac{V_{dc}}{L_f} \rangle_0 Kp_{id} & 0 \\ 0 & 0 & 0 \\ 0 & 0 & \langle \frac{V_{dc}}{L_f} \rangle_0 Kp_{iq} \\ 0 & 0 & 0 \end{bmatrix} \begin{bmatrix} -K_{i_{id}} \\ 0 \\ 0 \\ 0 \\ 0 \\ 0 \\ 0 \\ -\frac{R_f}{L_f} - \langle \frac{V_{dc}}{L_f} \rangle_0 Kp_{id} \\ 0 \\ -\omega + \langle V_{dc} \rangle_0 \omega \\ 0 \\ \frac{3}{2} \langle \frac{1}{CV_{dc}} \rangle_0 \langle V_{sd} \rangle_0 - \langle \frac{1}{CV_{dc}} \rangle_0 \langle 2R_f is_d \rangle_0 \end{bmatrix}$$

$$A = \begin{bmatrix} SL_f + R_f & 0 & -\omega L_f & 0 \\ 0 & SL_f + R_f + j0.6\omega L_f & 0 & -\omega L_f \\ \omega L_f & 0 & SL_f + R_f & 0 \\ 0 & \omega L_f & 0 & SL_f + R_f + j0.6\omega L_f \end{bmatrix}$$

$$K = \frac{3}{2} \alpha_G \begin{bmatrix} \langle V_{sd} \rangle_0 - \frac{\langle AR_f is_d \rangle_0}{3} & \langle V_{sd} \rangle_{0.6} - \frac{\langle AR_f is_d \rangle_{0.6}}{3} & \langle V_{sq} \rangle_0 & \langle V_{sq} \rangle_{0.6} \\ 0 & 0 & 0 & 0 \\ 0 & 0 & 0 & 0 \\ 0 & 0 & 0 & 0 \end{bmatrix}$$

$$H = \frac{3}{2} \alpha_G \begin{bmatrix} \langle is_d \rangle_0 & \langle is_d \rangle_{0.6}^* & \langle is_q \rangle_0 & \langle is_q \rangle_{0.6}^* \\ \frac{2}{3\alpha_G} & 0 & 0 & 0 \\ 0 & \frac{2}{3\alpha_G} & 0 & 0 \\ 0 & 0 & 0 & 0 \end{bmatrix} B = \begin{bmatrix} \beta & 0 \\ 0 & \beta \end{bmatrix} D = \begin{bmatrix} d & 0 \\ 0 & d \end{bmatrix}$$

$$B1_{DP} = [b1 \quad b2]$$

$$A1 = \begin{bmatrix} 0 & 0 & 0 & 0 \\ 0 & -j0.6\omega & 0 & 0 \\ 0 & 0 & 0 & 0 \\ 0 & 0 & 0 & -j0.6\omega \\ 0 & 0 & 0 & 0 \\ 0 & 0 & 0 & 0 \\ 0 & 0 & 0 & 0 \\ \langle \frac{V_{dc}}{L_f} \rangle_0 & 0 & 0 & 0 \\ 0 & \langle \frac{V_{dc}}{L_f} \rangle_0 & 0 & 0 \\ 0 & 0 & \langle \frac{V_{dc}}{L_f} \rangle_0 & 0 \\ 0 & 0 & 0 & \langle \frac{V_{dc}}{L_f} \rangle_0 \\ 0 & 0 & 0 & 0 \\ Kp_{iq} + \frac{K_{i_{iq}}}{s} & 0 & 0 & 0 \\ 0 & Kp_{iq} + \frac{K_{i_{iq}}}{s+j0.6\omega} & 0 & 0 \end{bmatrix}$$

Appendix B: Eigenvalue dq-dynamic phasor model

	$\langle \Delta x_1 \rangle_0$	$\langle \Delta x_1 \rangle_{0.6}$	$\langle \Delta x_2 \rangle_0$	$\langle \Delta x_2 \rangle_{0.6}$	$\langle \Delta x_3 \rangle_0$	$\langle \Delta x_3 \rangle_{0.6}$	$\langle \Delta x_4 \rangle_{0.6}$	$\langle \Delta is_d \rangle_0$	$\langle \Delta is_d \rangle_{0.6}$	$\langle \Delta is_q \rangle_0$	$\langle \Delta is_q \rangle_{0.6}$	$\langle \Delta V_{dc} \rangle_0$
Mode 1	0.00%	0.00%	0.00%	63.36%	0.00%	0.02%	0.02%	63.36%	79.13%	79.13%	89.60%	89.60%
Mode2	79.14%	79.21%	79.56%	35.37%	0.00%	77.37%	77.37%	35.34%	0.00%	0.00%	0.00%	0.00%
Mode3	0.00%	0.00%	0.00%	31.42%	0.00%	6.80%	6.80%	31.37%	39.25%	39.19%	44.40%	44.40%
Mode4	0.40%	0.32%	0.02%	53.37%	0.00%	0.02%	0.02%	53.37%	0.00%	0.00%	0.00%	0.00%
Mode5	9.85%	9.86%	9.90%	0.00%	99.50%	9.63%	9.63%	0.00%	0.00%	0.00%	0.00%	0.00%
Mode6	0.00%	0.00%	0.00%	21.23%	0.00%	0.00%	0.00%	21.23%	0.00%	0.00%	0.00%	0.00%
Mode7	42.02%	42.06%	42.25%	0.00%	0.00%	41.08%	41.08%	0.00%	0.00%	0.00%	0.00%	0.00%
Mode8	0.00%	0.00%	0.00%	0.00%	0.00%	14.75%	14.75%	0.00%	1.71%	1.71%	0.00%	0.00%
Mode9	7.32%	6.68%	0.00%	21.32%	0.00%	0.00%	0.00%	21.23%	23.45%	23.45%	0.00%	0.00%
Mode10	0.01%	0.01%	0.01%	0.09%	0.00%	16.70%	16.70%	0.04%	33.09%	33.16%	0.06%	0.06%
Mode11	49.34%	48.75%	42.25%	0.09%	0.00%	41.08%	41.08%	0.00%	23.45%	23.45%	0.00%	0.00%
Mode12	0.98%	0.99%	0.99%	0.01%	9.95%	0.51%	0.51%	0.01%	0.01%	0.01%	0.01%	0.01%